

Robust VAR Capability Curve of DER with Uncertain Renewable Generation

Aditya Shankar Kar¹, Kiran Kumar Challa¹, Alok Kumar Bharati², Ankit Singhal³, Venkataramana Ajjarapu¹

¹Department of Electrical and Computer Engineering, Iowa State University, IA, USA

²Pacific Northwest National Laboratory, Richland, WA, USA

³Department of Electrical Engineering, IIT Delhi, India

adityask@iastate.edu, kiranc@iastate.edu, ak.bharati@pnnl.gov, sankit@ee.iitd.ac.in, vajjarap@iastate.edu

Abstract—Active distribution system with high penetration of inverter based distributed energy resources (DER) can be utilized for VAR-related ancillary services. To utilize the DER flexibility, transmission system operator (TSO) must be presented with the aggregated DER flexibility of distribution system. However, the uncertainty in renewable generation questions the credibility of aggregated capability curve in practice. In this paper, we incorporate the uncertainty into aggregation process to develop a robust capability curve while preserving the real physics (unbalance and lossy nature) of distribution system. Statistical inference method is employed to quantify uncertainty in solar generation and quantified uncertainty is integrated into a chance constrained optimal power flow (OPF). It provides the grid operator with the dispatchable aggregated reactive power capability. The resulting capability curve with the associated probability can be harnessed by the TSO for decision making for both planning and operation.

Index Terms—VAR provision, Capability curve of distribution system, Optimal power flow, Distributed energy resources

I. INTRODUCTION

With an objective of achieving net zero emission by 2050, clean energy generation has gone through vital shift in favour of renewable energy resources [1]. Continuing the trend, penetration of renewable resources are projected to increase by 150% to serve 60% of midcontinent independent system operator (MISO) load in the coming decade [2]. Owing to the flexibility in size and process of installation, solar generation has taken significant portion of the projected clean energy production. Hence, the need for conventional synchronous machine based generation are reducing and existing conventional plants are getting retired [2]. Consequently, there is a decrease in the reactive power reserve, which is a reliable measure of the voltage stability margin [3], [4].

DER penetrated distribution system (D-system) is no longer a passive network as earlier and is capable of providing ancillary services to grid [5]–[7]. DERs can offer an alternative solution to the shortage of regional reactive power (VAR) availability. These geographically distributed DERs can be used in Volt/VAR control mode to provide both inductive and capacitive VAR [8], [9]. Deriving reactive power support from preinstalled DERs will be significantly cheaper compared to static VAR compensator. Also, the sheer scale of DERs in the D-system can enhance regional VAR availability and affect the voltage stability of electric grid positively. The aggregated capability of the DERs need to be communicated ahead of time

to the TSO by distribution system operator (DSO)/aggregator to be effectively utilized for voltage stability and flexibility.

In literature, the active power of DERs is aggregated for participating in wholesale energy and service energy markets [10]. However, our attention is directed at utilizing the DERs' VAR capabilities for enhancing performance of the power grid.

In this regard, a detailed frame work for VAR provisioning is given in [11]. Here, a day ahead aggregated VAR flexibility region (F-R) is derived to support the grid during disturbances [11].

Similarly in [12], authors have discussed about robust optimization based method to generate capability curve of active D-system without considering uncertainty in renewable generation. Active and reactive power capabilities of an active D-system are derived in [13], [14] assuming deterministic load and renewable generation. The capability curves derived in [11], [13], [14] are contentious as they overlook the inherent uncertainty associated with renewable sources.

In recent literature [15]–[17], few researchers have attempted to derive the capability of D-system including the uncertainty in renewable generation. In [15], uncertainty is included while deriving an aggregated active power capability of DER for real time market applications and does not provide any information on the VAR capability. In [16], uncertainty is considered in the maximum active power generation (P_{TVPP}^{gmax}) of a technical virtual power plant (TVPP). While deriving an aggregated active and reactive power capability region, the active power is assumed to be flexible in the range of 0 to P_{TVPP}^{gmax} . Since flexibility in reactive power [16] results in active power curtailment and consumer revenue, it is not in the best interests of consumers. A probable set of optimal aggregated reactive power curves are presented in [17]. The proposed method cannot be directly used by the TSO for decision making. The approach mentioned in [17] is computationally cumbersome with requirement of very high number of random samples. There are examples of solving probabilistic optimization models for accounting for renewable uncertainty

This paper is accepted for publication in IEEE PESGM 2024. The complete copyright version will be available in IEEE Xplore with published conference proceedings.

[18], [19], however, it is not feasible to employ these methods in practice due to various limitations.

To address the concerns mentioned in the previous paragraph, there is a need for robust VAR capability curve of a D-system. This curve should furnish a quantifiable numerical result of aggregated reactive power with associated confidence factor. In this paper, we define a robust VAR flexibility region (F-R) of D-system as $[\overline{Q}_{deamnd}^{sub}, \underline{Q}_{deamnd}^{sub}]$ at the substation (“ $\overline{Q}_{deamnd}^{sub}$ ” and “ $\underline{Q}_{deamnd}^{sub}$ ” represent maximum inductive and capacitive VAR support from D-system respectively).

DERs in D-system can be controlled to achieve aggregated reactive power demand in the F-R $[\overline{Q}_{deamnd}^{sub}, \underline{Q}_{deamnd}^{sub}]$. The novelty of the proposed method is summarized below:

- Uncertainty in solar power generation data [20] is quantified using statistical tools in a mathematically tractable way which can be incorporated into aggregation process.
- A credible DER VAR capability estimate is proposed which will quantify amount of aggregated reactive power ahead of time with given probability/risk factor so that the transmission operator can incorporate VAR capability into their decision-making algorithms. The proposed method ensures that the day ahead calculated aggregated reactive power will be dispatchable for service during the hour of operation.
- We utilized domain knowledge to reformulate the probabilistic optimization model via gaussian reformulation which is easier to solve.
- To establish a practically valid capability curve, we employ a 3-phase unbalanced D-system model, as unbalanced distribution of DERs can significantly affects the VAR capability. The determination of inverter size is guided by adherence to the IEEE 1547-2018 requirements.

II. QUANTIFICATION OF UNCERTAIN SOLAR GENERATION

The uncertainty in solar irradiance affects the generation of active power. Hence, it affects the amount of reactive power derived out of the DER. But from the grid operator prospective, uncertainty in reactive power generation needs to be quantified for operation and decision making.

In [20], hourly forecast data and actual data of solar generation for a year are presented for integration and operation study. We used historical data to quantify the error present in the forecast data. The objective is to create a model which will provide an expected value of the error for a given solar generation forecast, but not to upgrade the forecasting process. Finally for aggregation, it should be appropriate to use the forecast data in conjunction with the quantified uncertainty in terms of error in solar generation.

To create a model, errors in 8760 solar generation data points are required to be appropriately consolidated or grouped to provide information on errors for corresponding solar generation prediction value. Consolidation can be done in many ways. one of the consolidation methods is to group all the data that correspond to the same time of day. The primary

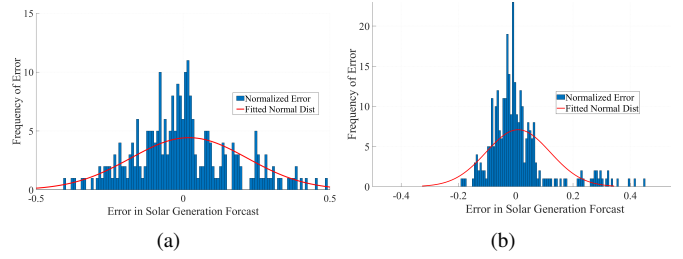


Fig. 1: Histogram and fitted normal distribution of the calculated error

drawback of this method is seasonal variation of the sunlight availability w.r.t time of day. Thus, it produces large variance. Instead, we observe the error in similar solar forecast value in the historical data. The confidence interval of error is much tighter in the later method compared to the previous one. Here, relative error is larger for lower generation forecast and it is smaller comparatively in case of large generation forecast. It signifies that absolute error magnitude remains similar to the prediction range. This can be considered as an indicator of accuracy of the prediction method and help operators to incorporate the quantified uncertainty in decision making.

Using the data in [20], error in forecast is calculated and the histogram can be plotted to observe its approximate distribution. In Fig.1(a) & 1(b), histogram of relative error is plotted for predicted generation percentage of 50% and 62.5% respectively. We observe histograms of errors to be close to both normal distribution as well as student’s t-distribution. As in most of the cases degree of freedom (number of observation) of error is more than 20, we fit the error to a normal distribution for the forecast values as shown in Fig.1. Details of relative error calculation (normalized error) with normal distribution fitting are articulated below.

- For accuracy, the night time data are removed where the forecasted value is zero.
- Normalize solar forecast value w.r.t the installed capacity.
- Calculate the absolute error and relative error w.r.t forecast value for all the data points.
- Group the similar normalized forecast value and their error together.
- Plot the histogram of relative error to see the distribution.
- Fit a normal distribution to the relative error and calculate the mean and standard deviation of the distribution.

In Table I, the mean (μ) and standard deviation (σ) of normal distribution is given for the relative error corresponding to predicted generation percentage of installed capacity for few cases.

III. SYSTEM MODELLING

Accuracy and validity of the capability curve for D-system depends entirely on its mathematical description. In the following section, model of inverter based DERs and linearized network are discussed with the pursuit of including them in the OPF formulation.

TABLE I: Quantified error in solar generation

| | Mean Error | Standard Deviation | Prediction Percentage |
|---|------------|--------------------|-----------------------|
| 1 | 0.2341 | 0.6543 | 0.0464 |
| 2 | -0.0169 | 0.5751 | 0.1234 |
| 3 | -0.0863 | 0.3702 | 0.2066 |
| 4 | 0.0044 | 0.4007 | 0.2936 |
| 5 | -0.0529 | 0.2629 | 0.3762 |
| 6 | -0.0299 | 0.2525 | 0.4598 |
| 7 | -0.0039 | 0.1598 | 0.5422 |
| 8 | 0.0083 | 0.1116 | 0.6260 |

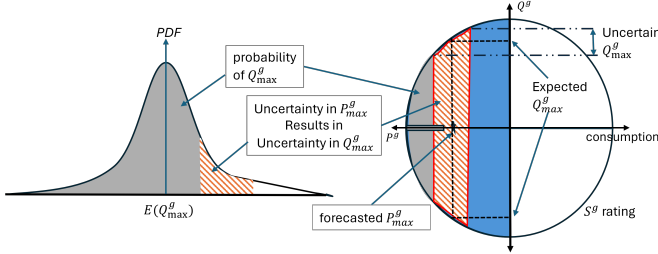


Fig. 2: Capability curve of inverter-based DER and Associated Uncertainty

A. Description of Hardware and their Limits

The P-Q capability of a single inverter can be plotted on a 2-D plane. If the x-axis represents the active power output and y-axis represents the reactive power output of the inverter, the capability curve can be represented as circle on P-Q plane as shown in Fig.2. Any point inside the boundary of the circle can be an operation point with appropriate control. However, the operating point is decided by the maximum active power output of DER. Depending on the active power output, the reactive power is limited due to the hardware limit of inverter of DER. As there is cost associated with the active power consumption, curtailing the active power may not be of interest for the owners of DERs.

But the recent IEEE 1547-2018 standard, mandates that DER must not deliver more than 90% of its KVA rating during operation. So, the DER can provide reactive power up to 44% of the inverter KVA rating to support the grid operation. Moreover, if the active power generation is lesser than more reactive power can be generated out of the IBRs as presented in Fig.2. Finally, operating point constraint is given in (1).

$$q_j^{g2} \leq S_j^{g2} - \tilde{p}_j^{g2} \quad (1)$$

where \tilde{p}_j^g represents uncertain solar generation p_j^g at node j .

B. Linear Model

A linear model of D-system is used in OPF formulation which is an extension of *LinDistFlow* to unbalance 3 phase circuit [11], [21]. The goal is to determine a linear relationship between the squared voltage term and power injection at D-system nodes to use in linear optimization. Applying KVL & KCL to the adjacent node of the 3phase unbalance network, we can write (2), where $P_j = [P_a P_b P_c]_j^T$ & $Q_j = [Q_a Q_b Q_c]_j^T$ represent the active and reactive power entering at node j for phase a, b, c and V_j represents the 3phase voltage vector for

node j . Z_{ij}^p and Z_{ij}^q are three phase impedance coefficient matrix of the line connecting node i & j .

$$V_i V_i^* = V_j V_j^* - Z_{ij}^p P_j - Z_{ij}^q Q_j \quad (2)$$

Using the connectivity matrix ' M ', we can represent (2) in compact form given in (3). The squared voltage term is written with the variable $Y_i = V_i V_i^*$.

$$[M_0 \quad M^T] [Y_0 \quad Y]^T = -Z_{ij}^p P_j - Z_{ij}^q Q_j \quad (3)$$

However, the voltage dependencies of the loads increase the complexity. Considering $a_{\phi,j}^0$ & $a_{\phi,j}^1$ are the fraction of load which are constant power and voltage dependent respectively at phase ϕ and node j . The load can be represented as

$$p_{\phi,j}^l(V_{\phi,j}) = p_{\phi,j}^l(a_{\phi,j}^0 + a_{\phi,j}^1 V_{\phi,j}^2) \quad (4)$$

Also, the difference in power entering at a node and leaving for connected adjacent node, can be equated to net load demand at each node. Net load is difference in load and generation at that node. This power balance is represented in (5).

$$\begin{aligned} MP &= p^g - (p^l a_{\phi,j}^0 + \text{diag}(p^l) Y a_{\phi,j}^1) \\ MQ &= q^g - (q^l a_{\phi,j}^0 + \text{diag}(q^l) Y a_{\phi,j}^1) \end{aligned} \quad (5)$$

Using (3) & (5) the expression of squared voltage is given in (6).

$$Y = K^{-1} [R^{eq}(p^g - p^l a_{\phi,j}^0) + X^{eq}(q^g - q^l a_{\phi,j}^0) - M^{-T} M_o Y_o] \quad (6)$$

Where

$$\begin{aligned} R^{eq} &= -M^{-T} Z_D^p M^{-1} \\ X^{eq} &= -M^{-T} Z_D^q M^{-1} \end{aligned} \quad (7)$$

$$K = I_{3N} + R^{eq} \text{diag}(p^l) a^1 + X^{eq} \text{diag}(q^l) a^1$$

C. Solar Generation with Associated Probability

Uncertainty in solar generation is quantified by associating the probability to the predicted values of solar power generation. The procedure followed in embedding this information into the reactive power capability curve of DER is explained in this section to provide more accurate and actionable information for TSO. Let us consider the DER capability as discussed in Section III-A. Taking the expected value on both sides of (1) and representing the entire formulation by an equivalent deterministic model, as in (8), is a convenient way to deal with uncertainty.

$$E(q_j^{g2}) \leq E(S_j^{g2} - \tilde{p}_j^{g2}) = S_j^{g2} - E(\tilde{p}_j^{g2}) \quad (8)$$

From Fig.2 and equation (1) & (8), it can be observed that, if the actual p_j^g is higher than $E(p_j^g)$ with positive error, then the room for maximum possible reactive power generation (q_j^g) at node j will be lesser than calculated value. On other hand, if the actual p_j^g goes below the $E(p_j^g)$, then the maximum possible q_j^g will be higher than calculated value. Hence the aggregated reactive power of D-system holds good, if $p_j^g < E(p_j^g)$ but it does not remain valid for $p_j^g > E(p_j^g)$. So with the expected value of $E(p_j^g)$, inequality in (8) holds good with probability of 0.5.

Validity of capability curve can be improved under uncertain scenario by including the chance constrained formulation given in (9). Essentially (9) ensures that hardware constrained (1) holds with a probability $1 - \alpha$ where α is the risk factor.

$$\mathbb{P}(q_j^{g2} \leq S_j^{g2} - \tilde{p}_j^{g2}) \geq 1 - \alpha \quad (9)$$

In practice, it is preferred to satisfy (9) for very high probability with lower (α) risk factor. Considering $\hat{p}_j^g = E(\tilde{p}_j^g) + \mu_{error} + \sigma_{error}$ and $\hat{p}_j^g = E(\tilde{p}_j^g) + \mu_{error} + 2\sigma_{error}$ respectively, we can ensure (9) with probability $\mathbb{P} = 0.84$ and $\mathbb{P} = 0.976$. For ensuring the validity of (9) with a probability of \mathbb{P} , the value of active power p_j^g should be considered according to (10).

$$\hat{p}_j^g = E(\tilde{p}_j^g) + \mu_{error} + z\sigma_{error} \quad (10)$$

where $z = \Phi^{-1}(\mathbb{P})$ and $\Phi(z) = \int_{-\infty}^z \frac{1}{\sqrt{2\pi}} e^{-\frac{x^2}{2}} dx$ represents the cumulative distribution function of the standard normal.

IV. OPF FORMULATION

VAR flexibility region (F-R) of a D-system can be defined as the maximum reactive power that can be absorbed (lagging VAR) or generated (leading VAR) by DERs. To calculate the available VAR F-R at the substation, we need to minimize and maximize the net VAR drawn from the substation. For a given solar generation p_j^g from inverter, we can use rest of VA capacity to generate the q_j^g . Adding the q_j^g at each node algebraically, can potentially violate the D-system constraint. Hence, an OPF is formulated to minimize and maximize the net VAR injection by D-system as given in (11a). The objective function (11a) is the difference between the VAR generation and demand at the D-system node. In this OPF formulation, the solar power generation, active and reactive power demand of load, are given as input and the reactive power generation q_j^g of individual DER is the output of the optimization module.

$$\min_{q_j^g} \sum_{i=1}^N q_j^g - \sum_{i=1}^N q_j^l \quad (11a)$$

$$\text{s.t. } Y = K^{-1}[R^{eq}(\tilde{p}^g - p^l a^0) + X^{eq}(q^g - q^l a^0) + 1v_0^2], \quad (11b)$$

$$\underline{y}_j \leq y \leq \overline{y}_j, \quad (11c)$$

$$p_j = \tilde{p}_j^g - p_j^l(a_j^0 + a_j^1 y_j), \quad (11d)$$

$$q_j = q_j^g - q_j^l(a_j^0 + a_j^1 y_j), \quad (11e)$$

$$\mathbb{P}(q_j^{g2} \leq S_j^{g2} - \tilde{p}_j^{g2}) \geq 1 - \alpha \quad (11f)$$

In the formulation, constraint (11b) is a linear function of squared voltage terms which represents 3-phase linearized power flow. The upper and lower bound of the each nodal voltage is set to 1.05 and 0.95 respectively in (11c). Active and reactive power balance in D-system are presented in (11d) & (11e). The hardware limits are given in (11f). Here, OPF is formulated with uncertain solar generation. With p_j^g is

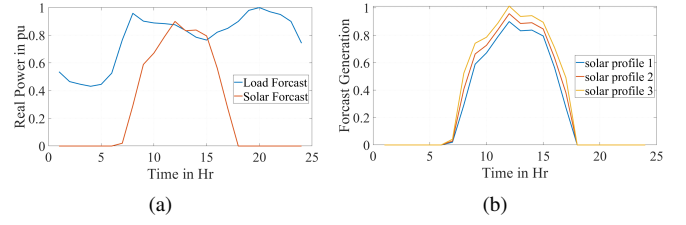


Fig. 3: (a) Day ahead load and solar generation forecast, (b) Generated solar profile with associated probability

represented as a random variable \tilde{p}_j^g , the constraint (11e) is modeled as chance constrained problem. However, for solving the optimization problem, solar power generation (\tilde{p}_j^g) with associated probability (\mathbb{P}) is calculated as described in (10). This \tilde{P}_j^g can be used to ensure equation (11f) with probability $\mathbb{P} \geq 1 - \alpha$. With all other deterministic parameters, we replace \tilde{p}_j^g with \hat{P}_j^g in (11b), (11d) for a Gaussian reformulation of OPF.

V. TEST SYSTEM DESCRIPTION AND RESULT

We have considered IEEE 123 node 3-phase unbalanced D-system with 3.5 MW demand. Solar generation penetration is considered as 90% of the peak load. Equal capacity of DERs are connected at all the nodes in D-system. Inverter ratings are considered to be 10% higher than the peak solar generation level to be consistent with IEEE-1547. The solar and load profiles for 24 hours are given in Fig.3(a).

As discussed in section II, we have quantified the error in solar power prediction to be Gaussian distribution representing the error in terms of mean error and standard deviation. The deterministic solar generation profile presented in Fig.3(a), is considered as the expected solar generation value for 24 hour. Matching it with the prediction percentage of Table I, the mean error and its associated stand deviation is decided. For desired probability value " \mathbb{P} " ($\mathbb{P} = 0.84$ and $\mathbb{P} = 0.976$), the synthetic solar power generation generation profile is created using (10) as shown in Fig.3(b). The forecasted solar power generation is presented as solar profile 1. Solar profile 2 and solar profile 3 are calculated with associated probability $\mathbb{P} = 0.84$ and $\mathbb{P} = 0.976$.

The solar generation profiles presented in Fig.3(b) are used for solving the Gaussian reformulated OPF [15]. As the formulated OPF is convex with linear constraints and objective function, it can be solved efficiently using the standard routines. The resulting aggregated capability curve of D-system is presented in Fig.4, where the flexibility region 1 (F-R1), F-R2, F-R3 corresponds to the solar profile 1, 2, 3 respectively. Hence, the probability of F-R remaining valid, can be attributed to the probability (\mathbb{P}) associated with the synthetic solar profile. The aggregated F-R2 and F-R3 are valid with the probability of 0.84 and 0.97 respectively. With the dotted line in Fig.4 as a base load, the D-system can be operated with in the shaded region. During the nighttime, as the solar generation is absent, we are certain about the VAR capability curve of D-system. With the variation in solar

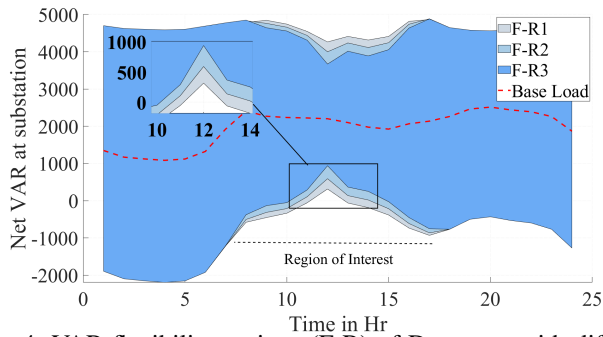


Fig. 4: VAR flexibility regions (F-R) of D-system with different probability

generation during the day, VAR capability curve of D-system changes. Hence, day time of capability curve is region of interest as shown in Fig.4. The aggregated capability curve during the period of interest, is presented in Table II with the associated probability. The maximum and minimum operating points are indicated with respect to time of the day for the predicted load and solar generation. The -ve VAR in Table II, can be considered as the reactive power injection from the D-system to the transmission system (T-system). In Table II, the variation in Q_{min}^{sub} at 12th hour is 624 (939-315=624) VAR for a single distribution network. However, as seen by the TSO, this variation due to uncertainty will be multi-fold with 10s to 100s distribution networks downstream at a given T-system.

TABLE II: Aggregated capability curve of the D-system

| hr | Base case P=0.5 | | P=0.86 | | P=0.97 | |
|----|-----------------------|-----------------------------|-----------------------|-----------------------------|-----------------------|-----------------------------|
| | \bar{Q}_{max}^{sub} | $\underline{Q}_{min}^{sub}$ | \bar{Q}_{max}^{sub} | $\underline{Q}_{min}^{sub}$ | \bar{Q}_{max}^{sub} | $\underline{Q}_{min}^{sub}$ |
| 6 | 4691 | -1923 | 4691 | -1923 | 4691 | -1923 |
| 7 | 4762 | -1210 | 4768 | -1213 | 4777 | -1204 |
| 8 | 4788 | -578 | 4834 | -503 | 4851 | -375 |
| 9 | 4846 | -452 | 4762 | -313 | 4645 | -132 |
| 10 | 4742 | -335 | 4660 | -210 | 4557 | -50 |
| 11 | 4546 | -55 | 4438 | 106 | 4311 | 290 |
| 12 | 4264 | 315 | 3998 | 591 | 3670 | 939 |
| 13 | 4413 | -61 | 4237 | 137 | 4015 | 367 |
| 14 | 4315 | -185 | 4114 | 19 | 3888 | 250 |
| 15 | 4411 | -383 | 4243 | -215 | 4056 | -25 |
| 16 | 4817 | -734 | 4739 | -611 | 4637 | -451 |
| 17 | 4865 | -930 | 4886 | -863 | 4882 | -752 |
| 18 | 4648 | -766 | 4648 | -766 | 4648 | -766 |

VI. DISCUSSION AND CONCLUSION

In this paper, we have presented a methodology for including uncertainty in the DER aggregation process. The resulting aggregated capability curve is expected to remain valid during uncertain solar generation scenarios. The information from Table II (communicated a day ahead to TSO) along with current solar insolation measurements will help TSO in making a confident decision to request a certain amount of VAR from DSO. The robust capability curve will be essential as the variation due to uncertainty is large. In absence of uncertainty consideration, the TSO cannot make a confident decision. A robust capability curve will provide opportunity for TSO to enhance the efficiency of the transmission system and congestion management during normal operation. It also enables

effective reactive power management during contingencies. As the unbalance in D-system and inverter sizing are considered in aggregation process, the developed aggregated capability curve will be dependable for TSO & DSO decision making. This additional knowledge of aggregated DER capability enables utilities for peak VAR management. In future work, we plan to include the uncertainty in load in active distribution and operating condition of DERs.

REFERENCES

- [1] P. Denholm, P. Brown, W. Cole, T. Mai, B. Sergi, M. Brown, P. Jadun, J. Ho, J. Mayernik, C. McMillan, and R. Sreenath, "Examining supply-side options to achieve 100
- [2] "Miso 2022 regional resource assessment a reliability imperative report," 2022. [Online]. Available: <https://www.misoenergy.org/planning/policy-studies/RRA>
- [3] B. Park, S. Im, D. Kim, and B. Lee, "Clustered effective reactive reserve to secure dynamic voltage stability in power system operation," *IEEE Transactions on Power Systems*, vol. 36, pp. 1183–1192, 3 2021.
- [4] B. Leonardi and V. Ajjarapu, "Investigation of various generator reactive power reserve (grpr) definitions for online voltage stability/security assessment," 2008.
- [5] A. O. Rousis, D. Tzelepis, Y. Pipelzadeh, G. Strbac, C. D. Booth, and T. C. Green, "Provision of voltage ancillary services through enhanced tso-dso interaction and aggregated distributed energy resources," *IEEE Transactions on Sustainable Energy*, vol. 12, pp. 897–908, 4 2021.
- [6] E. O. Kontis, A. R. D. Nozal, J. M. Mauricio, and C. S. Demoulias, "Provision of primary frequency response as ancillary service from active distribution networks to the transmission system," *IEEE Transactions on Smart Grid*, vol. 12, pp. 4971–4982, 11 2021.
- [7] A. K. Bharati, V. Ajjarapu, W. Du, and Y. Liu, "Role of distributed inverter-based-resources in bulk grid primary frequency response through helics based smtd co-simulation," *IEEE Systems Journal*, vol. 17, no. 1, pp. 1071–1082, 2023.
- [8] H. Zhu and H. J. Liu, "Fast local voltage control under limited reactive power: Optimality and stability analysis," *IEEE Transactions on Power Systems*, vol. 31, pp. 3794–3803, 9 2016.
- [9] A. Singhal, V. Ajjarapu, J. Fuller, and J. Hansen, "Real-time local volt/var control under external disturbances with high pv penetration," *IEEE Transactions on Smart Grid*, vol. 10, pp. 3849–3859, 7 2019.
- [10] M. D. Somma, G. Graditi, and P. Siano, "Optimal bidding strategy for a der aggregator in the day-ahead market in the presence of demand flexibility," *IEEE Transactions on Industrial Electronics*, vol. 66, pp. 1509–1519, 2 2019.
- [11] A. Singhal, A. K. Bharati, and V. Ajjarapu, "Deriving ders var-capability curve at tso-dso interface to provide grid services," *IEEE Transactions on Power Systems*, vol. 38, pp. 1818–1831, 3 2023.
- [12] X. Chen and N. Li, "Leveraging two-stage adaptive robust optimization for power flexibility aggregation," *IEEE Transactions on Smart Grid*, vol. 12, pp. 3954–3965, 9 2021.
- [13] J. Silva, J. Sumaili, R. J. Bessa, L. Seca, M. A. Matos, V. Miranda, M. Caujolle, B. Goncer, and M. Sebastian-Viana, "Estimating the active and reactive power flexibility area at the tso-dso interface," *IEEE Transactions on Power Systems*, vol. 33, pp. 4741–4750, 9 2018.
- [14] T. Zhang, J. Wang, H. Wang, J. Ruiyang, G. Li, and M. Zhou, "On the coordination of transmission-distribution grids: A dynamic feasible region method," *IEEE Transactions on Power Systems*, vol. 38, pp. 1855–1866, 3 2023.
- [15] Y. Zhang, S. Shen, and J. L. Mathieu, "Distributionally robust chance-constrained optimal power flow with uncertain renewables and uncertain reserves provided by loads," *IEEE Transactions on Power Systems*, vol. 32, no. 2, pp. 1378–1388, 2017.
- [16] Z. Tan, H. Zhong, Q. Xia, C. Kang, X. S. Wang, and H. Tang, "Estimating the robust p-q capability of a technical virtual power plant under uncertainties," *IEEE Transactions on Power Systems*, vol. 35, pp. 4285–4296, 11 2020.
- [17] P. Goergens, F. Potratz, M. Gödde, and A. Schnettler, "Determination of the potential to provide reactive power from distribution grids to the transmission grid using optimal power flow," pp. 1–6, Sep. 2015.

- [18] C. Zhang, H. Chen, K. Shi, Z. Liang, W. Mo, and D. Hua, "A multi-time reactive power optimization under interval uncertainty of renewable power generation by an interval sequential quadratic programming method," *IEEE Transactions on Sustainable Energy*, vol. 10, pp. 1086–1097, 7 2019.
- [19] S. Stanković and L. Söder, "Probabilistic reactive power capability charts at dso/tso interface," *IEEE Transactions on Smart Grid*, vol. 11, pp. 3860–3870, 9 2020.
- [20] Y. Z. [https://www.nrel.gov/grid/solar-power data.html](https://www.nrel.gov/grid/solar-power-data.html), "Solar power data for integration studies," pp. 3860–3870.
- [21] D. B. Arnold, M. Sankur, R. Dobbe, and K. Brady, *Optimal Dispatch of Reactive Power for Voltage Regulation and Balancing in Unbalanced Distribution Systems*. IEEE PESGM 2016 Boston, 2016.